Revista Brasileira de Meteorologia, v.15, n.2, 45-56, 2000

BAROTROPIC INSTABILITY, TROPICAL HEATING AND THE SOUTHERN HEMISPHERE INTRASEASONAL VARIABILITY

MARCELO BARREIRO
Instituto de Fisica, Facultad de Ciencias, Universidad de la Republica., Montevideo, Uruguay
Texas A&M Univercity - Departament of Oceanography College Station , Texas 77843-3146 - USA
marcelo@ocean.tamu.edu

GABRIEL PISCIONATTO
Instituto de Mecanica de los Fluidos e Ingenieria Ambiental,
Facultad de Ingenieria IMFIA, Universidad de la Republica, Montevideo, Uruguay
gabrielp@fing.edu.uy

ABSTRACT

The mechanisms for intraseasonal variability of the southern hemisphere (SH) winter are studied using a nonlinear non-divergent barotropic potential vorticity model on the sphere. The possibility of low frequency unstable modes induced by topography is examined to compare with the northern hemisphere (NH) case. According to this simple model for the SH winter the most important mechanism in creating intraseasonal oscillations is the barotropic instability of the non-zonal flow, while the topography, which seems to be essential in the NH, plays here a secondary role. The influence of the Madden Julian Oscillation on the intraseasonal mode induced by the barotropic instability of the non zonal flow is also studied by means of a highly idealized vorticity source. It is found that for realistic heating values both signals coexist, suggesting a mechanism of creation of interannual variability due to the nonlinear coupling of the frequencies involved.

key-words: barotropic instability, topographic instability, intraseasonal

RESUMO : INSTABILIDADE BAROTRÓPICA, AQUECIMENTO TROPICAL E OSCILAÇÃO.
No presente trabalho, são estudados os mecanismos de geração de variabilidade intrasazonal do Hemisferio Sul (HS) mediante o uso de um modelo de vorticidade. Encontra-se que, no caso do inverno do HS, o mecanismo mais importante é a instabilidade barotrópica de fluxo não-unidirecional, enquanto a topografia essencial no Hemisferio Norte tem aqui um papel secundário. Igualmente, é estudada a influência da oscilação de Madden-Julian sobre o modo intra-sazonal induzido, encontrando-se que, para valores realistas, existem os dois sinais, agindo como mecanismo de criação de variabilidade intra-anual por causa do acoplamento não-linear entre eles.

Palavras-chave: Instabilidade barotrópica, instabilidade topográfica, intra-sazonal.

1. INTRODUCTION

We study the atmospheric intraseasonal variability of the Southern Hemisphere (10-100 days) which, like others aspects of its circulation, has been studied less than others regions of the planet. Since the discovery of the 40-50 day oscillation (MJO) in the tropics by Madden and Julian (1971), there has been a considerable effort in attempting to understand the low frequency regimes in the tropics and its relationship with its counterparts in the extratropics.

Extratropical evidence of low frequency variability between 40 and 50 days in observations as well as in computer simulations has been found in both hemispheres by many authors (e.g. Dickey et al. 1991, Ghil and Mo 1991a,b). It was also found that the signal of the 40 days oscillation is strongest in the winter season of either hemisphere (Ghil and Mo 1991b, GM hereafter).

Many possibilities for the dynamical origin of the middlatitude low frequency variability (LFV) have been proposed for the Northern Hemisphere case. Rosen and Salstein (1983) suggest the tropical forcing as the main

cause of the observed oscillation. Simmons et al (1983) advanced the hypothesis that perhaps the most important part of the LFV could be attributed to the barotropic instability of non-zonal climatological flow. They also suggested that the basic flow could be maintained by topography and vorticity forcing in a nonlinear barotropic model. Jin and Ghil (1990) demonstrated the relevance of the oscillatory topographic instability in β-plane models with a sufficient number of meridional modes.

Strong et al. (1993, hereafter SJG) studied the influence of topographically forced nonlinear resonance, the origin of multiple equilibria and LFV in a barotropic model, as well as the influence of the tropical oscillation (MJO) on it. They concluded, in the context of their model, that for the NH the presence of topography is totally necessary for the development of intraseasonal modes, and that tropical and extratropical oscillations can be viewed as essentially independent phenomena, but with a resonant response of the extratropical signal to the tropical one.

As can be seen, while the NH has been studied in great detail, the SH has not. It is the purpose of this work then, to clarify the role of the topography and of the tropical heating on the LFV of the SH winter following the same treatment used by SJG, i.e. to study the self-maintaining oscillations in the framework of a forced nonlinear barotropic model.

Moreover, we will try to recover some of the low frequency observed patterns of the SH. The recognition of the preferred modes of circulation of the extratropical SH atmosphere and, in general, the better understanding of its low frequency variability has as main purpose the extension of the numerical weather prediction into the medium and low frequency ranges (>10 days) because it has been recognized as the major modulator of synoptic scale events.

It is interesting to point out that the intraseasonal variability of the SH atmospheric circulation has been found to be more complex than that of the NH on both its spatial structure and temporal behavior (GM). This greater complexity has been attributed to the less dominant role of the topography in the dynamics of the atmosphere, as well as to the larger wavenumber in land-sea temperature contrast (three instead of two).

The work is organized in the following way. The model used is described in section 2. In section 3 the steady-state solutions are obtained. The cases with and without topography are treated separately to study the role of topographic instability in the dynamics. In section 4 a linear stability analysis of the solutions of the previous section is performed. The asymptotic time depcndcnt solutions are computed in section 5, where the possible influence of the MJO on them is studied. Section 6 contains a summary of the results.

2. MODEL DESCRIPTION

a. Equation and parameter values.

The atmospheric model used is governed by the equivalent-barotropic form of the equation for the conservation of potential vorticity on the sphere which, written in a nondimensional form, becomes (SJG)

$$\frac{\partial}{\partial t}(\Delta - \Gamma^2)\psi + J[\psi, \Delta\psi + 2\mu(1+h)] = \alpha\Delta(\rho^*\psi^* - \psi) - \nu\Delta^3\psi \qquad (1)$$

In Eq.(1) ψ is the horizontal streamfunction, Δ the horizontal Laplacian, J the Jacobian operator, h is the topographic height, and μ the sine of latitude. The right hand side of Eq. (1) induces a relaxation of the flow, supposing an hypothetical Ekman layer, towards the flow represented by the forcing streamfunction ψ^* with a characteristic time scale α^{-1}=10 days. ψ^* represents the climatological background SH wintertime circulation and results from the combined effects of synoptic eddy fluxes, differential heating and baroclinic dynamics. The strength of ψ^* is given by the nondimensional number $\rho^* = U^*/a\Omega$ whose magnitude can be related to the effect of an "external" forcing which maintains the structure of ψ^* but changes its intensity. We take ρ^* as a control parameter of our system and show that depending on its value the behavior of the model can be quite different.

Γ is the external Rossby radius of deformation with a dimensional value of 1100 km, which is an interpolation between an internal baroclinic Rossby radius and the barotropic one (Legras and Ghil 1985).

Equation (1) is discretized using the spherical spectral transform method with a triangular truncation T21. We consider symmetry of the flow about the Equator as in SJG, which yields the number of real modes to be 231. In order to take into account not resolved scales a very small viscous term is added and its coefficient ν taken such that the smallest mode of truncation has a damping rate of (10 days)$^{-1}$.

The topography used is real topography of the SH obtained form the European Center of Medium Weather Forecast (ECMWF), and a scale height of H=9 km for the troposphere is taken. Clearly, due to the low resolution

of the truncation T21 used, the topography is much more smoothed than the real one and sharp features like the Andes are not resolved quite correctly. However, it is seen that topography is totally different from the NH one (see Fig.(1)); here the most part of the topography is located zonally at the Antarctica which acts as a wall for the flow. The Andes and it counterparts in Africa seem to be too low to be important in the dynamics of the system as represented in this model, in which, topographical effects are limited to the direct influence of h on the nonlinear term of the mechanical budget of vorticity.

As discussed above, we will concentrate only in the month of July, which we consider representative of the SH winter. This interpretation is supported by the work of Mechoso et al (1991), which found that the leading Empirical Orthogonal Functions (EOF) at 500 mb showed barotropic structure and exhibit no preference for early, middle or late winter. The forcing streamfunction $\psi^*(\phi,\mu)$ used in this study was calculated in the

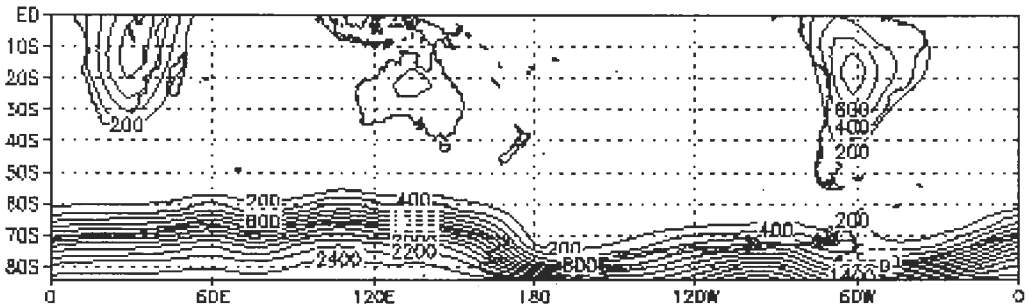

Fig. 1- Southern hemisphere topography used in the model. Note that due to the T21 resolution used the topography is very smooth. Contours are in meters.

following way. First the climatological streamfunction was calculated from the climatological flow at 300 mb for the years 1975-83 obtained from the ECMWF (see Fig.(2)). Then, to obtain the forcing streamfunction ψ^* we impose the climatology to be a stationary solution of Eq.(1). This is done having in mind, as was shown by Andrews (1984), that the detailed structure of the forcing which maintains the basic state may alter the stability properties of the field. However, we opted to follow the work of Li and Nathan (1997) and the forcing is computed by specifying first the basic state by some climatological streamfunction. It must be noted that the resulting forcing streamfunction is zonally asymmetric, a remarkable difference from the work of SJG.

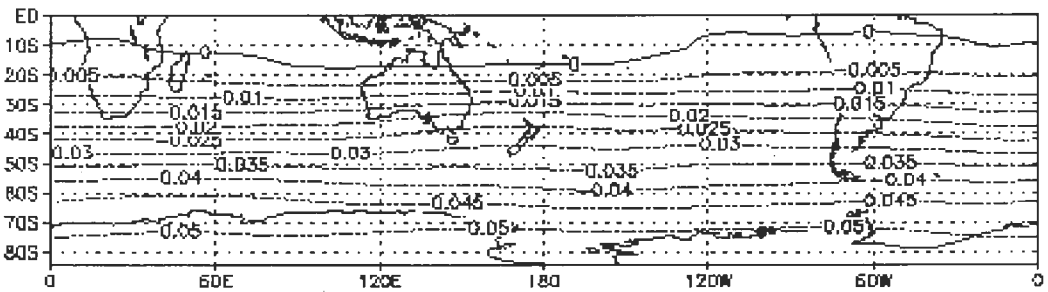

Fig. 2- Non-dimensional climatological 300mb streamfunction for July.

b. Tropical forcing

The potential influence of the Madden-Julian oscillation on the extratropical weather has been recognized by several works (e.g, Lau and Phillips 1986), but it is not yet clearly established the existence of a connection between it and the intraseasonal oscillations of the SH. The arguments (also valid for the NH) have been the insufficient amount of data in observational studies and the fact that the impact of the tropical anomalies is expected to be modest in comparison with the intrinsic variability in midlatitudes (Blade and Hartmann 1995).

In order to investigate the behavior of our simple model in the presence of an anomalous tropical heating, we introduce on the right hand side of Eq.(1) a vorticity

stretching source of the form

$$Q = \delta f_0 D \qquad (2)$$

where f_0 is the Coriolis parameter, D the divergence of the field and δ a control parameter which takes into account the intensity of the heating. The advection of absolute vorticity by the divergent component of the wind has also been shown to be an important vorticity source (Grimm and Silva Dias 1995). However, we model the heat source in the simplest possible way in order to compare our results with the work of SJG. As in SJG we consider $f_0 \sim 10^{-5}\ s^{-1}$ and $D \sim 10^{-6}\ s^{-1}$ which yield $Q \sim 10^{-11}\ s^{-2}$ (δ=1). The source was located between $\pm 10^0$ latitude and 80^0 E-160^0 E longitude and propagates eastward between its boundaries in the form of an oscillatory dipole, a necessary requirement to achieve a realistic heating field. We allow the source to oscillate with periods of T = 30, 40 and 50 days to explore a possible sensitivity of the flow.

3. STEADY STATE SOLUTIONS

As a first step we consider the study of the steady state solutions of the equation (1) and their dependence on the intensity of the forcing ρ^*. Steady states are found using the arc-length continuation method described in Kubicek and Marek (1983). In order to characterize the different solutions we calculate the total energy E=K+P, where $K = -\iint \psi \Delta \psi d\mu d\phi$ is the kinetic energy and $P = \iint \Gamma^2 \psi^2 d\mu d\phi$ is the potential energy associated with the free surface displacement. A representative measure of the behaviour of the model is shown in bifurcation diagrams where the energy E normalized by the corresponding forcing value ρ^* is ploted as a function of ρ^*. In these diagrams turning points represent saddle-node bifurcations in which a new pair of stationary solutions are created. Each turning point has associated another turning point in which an inverse saddle-node bifurcation accurs where the points colide and dissapear.

a. Case I: with topography.

We let the forcing intensity to vary in the range $0.6 \leq \rho^* \leq 2.0$; the results are shown in Fig.(3a). It can be seen that for values of the forcing intensity less than 1.5 only one stationary solution exists, while from this point up to $\rho^* = 1.85$, multiple solutions exist. The first turning point appears at about $\rho^* = 1.67$ and in this region the curve shows a complicated structure with several folds. Previous to this point the curve shows a smooth character having two folds for values of the forcing parameter near 1.1 and 1.3. In the region of the parameter forcing between 1.5 and 1.85 there exist 3, 5 or 7 different steady state solutions of the model for the same control parameter value. The difference among the energies of the different regimes is very small and the structure of the associated flows with each one of this multiple equilibria are very similar (not shown).

b. Case II: without topography.

To analyze the role of topography in the dynamics of the model we repeat the solution of case I, but with flat topography. It can be clearly seen from Fig.(3b) that although the curve has one fold for ρ^*=1.3, it is a totally smooth one and it does not present as many multiple equilibria as in case I, existing a region of multiple solutions in a very narrow band only for very strong parameter values (ρ^*>2). This states clearly that the role of topography in the dynamics of our model is that of favoring the appearance of multiple steady solutions, i.e., it complicates the picture allowing 'a priori' the atmosphere to change among different regimes.

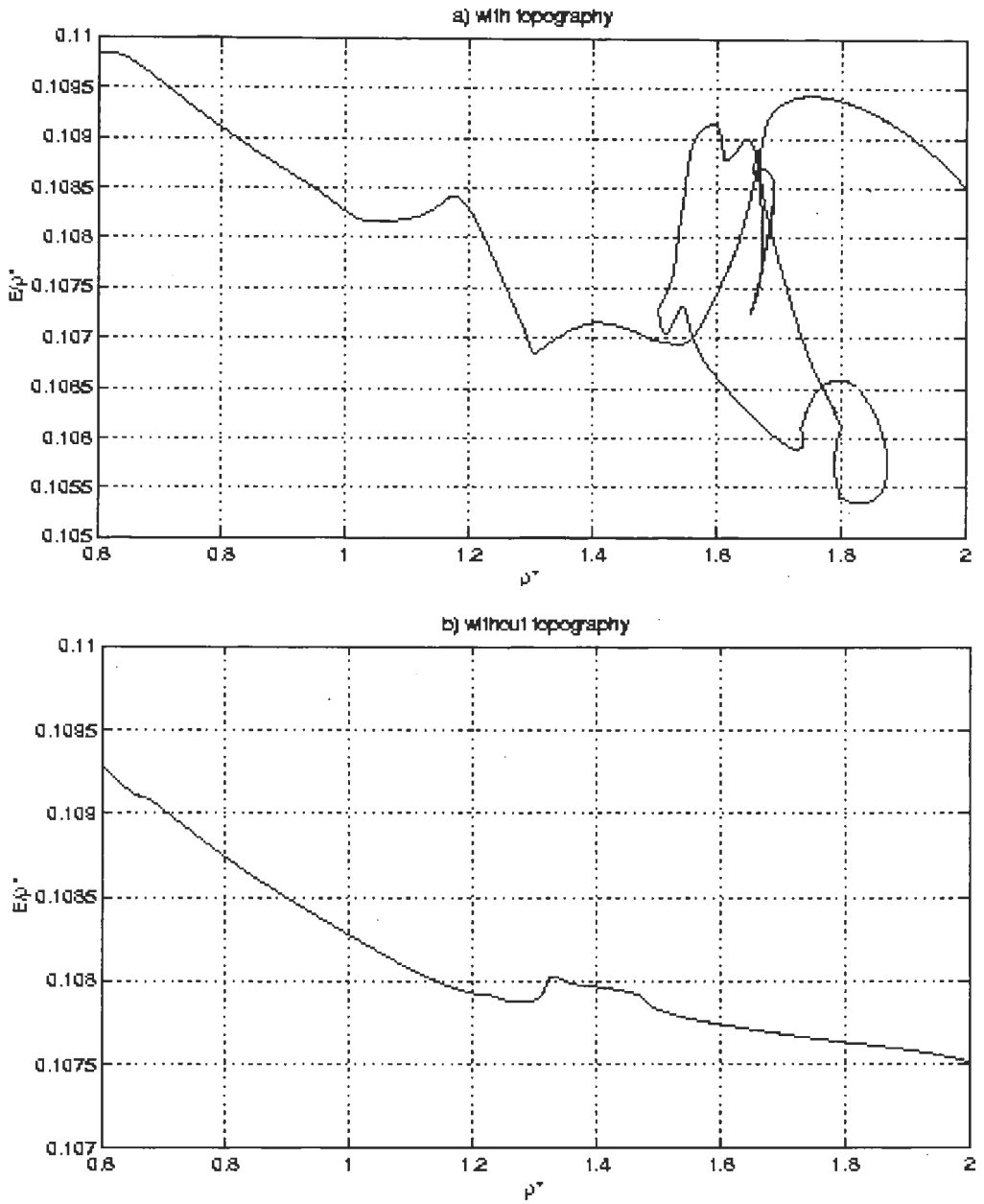

Figure 3- Dependence of the steady state solutions on the forcing parameter ρ^* (see text for explanation) in the range $0.6 \leq \rho^* \leq 2.0$, a) when topography is included and b) when topography is absent.

4. LINEAR STABILITY ANALYSIS

Linear stability analysis of the stationary solutions Ψ_S found in section III is performed here by examining the spectrum of eigenvalues λ of the linear operator L_S associated to Eq. (1) expanded as a function of a small time dependent perturbation ψ' in the neighborhood of Ψ_S. We look for possible Hopf bifurcations (Guckenheimer and Holmes 1983) in which stationary solutions lose their stability and periodic solutions are created. These bifurcations are recognized in the eigenvalue spectrum by the crossing of the imaginary axis by a pair of complex conjugate eigenvalues from the left into the rigth half-plane.

For the case with topography the results show the existence of distinct regimes depending on the control parameter values. For $\rho^* \leq 0.92$, the single steady state solution shown is linearly stable. At this point, a pair of

complex conjugate eigenvalues cross the imaginary axis, leading to an oscillatory solution with period $T = 2\pi / \mathrm{Im}(\lambda)\Omega$ near the 30 days and e-folding time $(= 1/2\pi\ \mathrm{Re}(\lambda))$ equal to 350 days. The instability persist from this value and up to ρ^*=1.02 (see figure 4). This unstable mode has very large values of e-folding times, being the smallest one of about 100 days and with a period of nearly 34 days for $\rho^* \cong 0.98$. Moreover, for $\rho^* = 1.0$ the period is around 36 days and the e-folding time increases to 125 days.

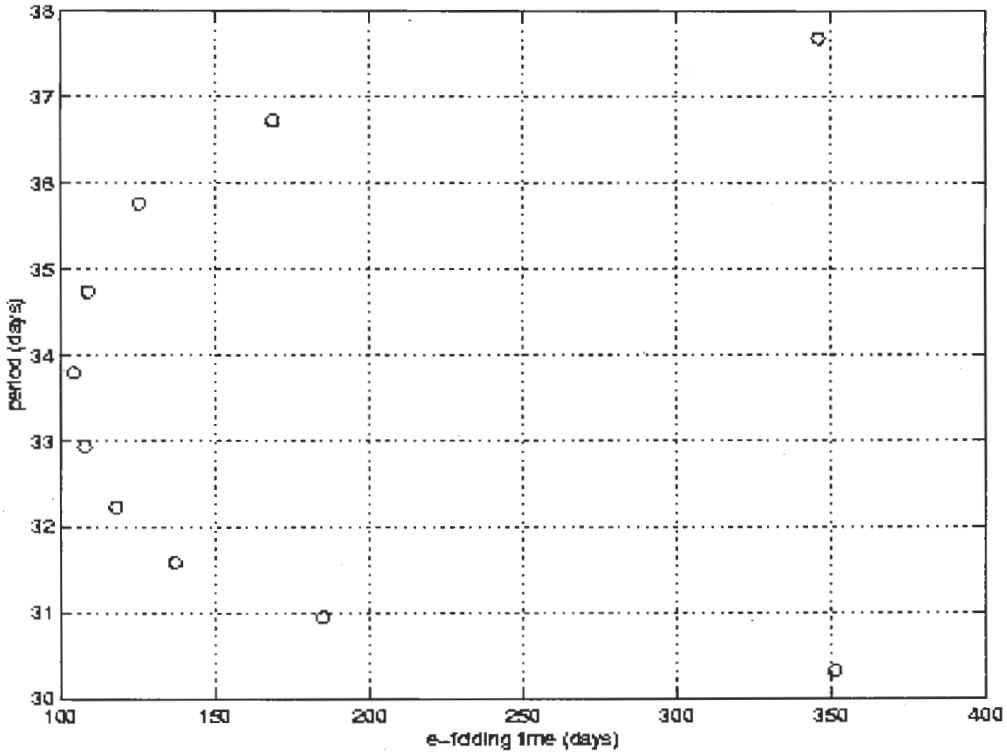

Figure 4- Evolution of eigenvalues for the unstable mode as a function of ρ^* for the range $0.92 \leq \rho^* \leq 1.02$. Coordinates of points are given in period vs e-folding time (see text).

For $\rho^* \in [1.02, 1.28]$ the soluton is linearly stable, up to $\rho^* = 1.28$ where it becomes unstable again because of a Hopf bifurcation. If we continue to increase the forcing, two new complex conjugate eigenvalues cross the imaginary axis at $\rho^* \cong 1.43$, and two more at $\rho^* \cong 1.47$, allowing the system to present aperiodic or chaotic solutions.

In order to clarify the origin of the intraseasonal mode found in the realistic range of ρ^*, i.e whether it is or not induced by topographic instability, we perform the eigenanalysis with flat topography. The results show that the window of instability still exist for values of the forcing parameter ρ^* between 0.92 and 1.11, almost equal to the case with topography. Moreover, the unstable mode has the same period and e-folding time as before (not shown). Thus, we can not attribute the intraseasonal oscillation found for the SH winter to the topographic instability mechanism, in contrast with the NH winter case in which, as was found in the work of SJG, the lack of topography eliminates completely the intraseasonal mode.

To inspect the spatial structure of the intraseasonal mode an eigenvector analysis was also performed. Fig. (5) shows the spatial patterns of different phases for half of the cycle of the unstable mode for $\rho^* = 1$ and fig. (6) shows the Hovmoller diagram. Both figures show that the intraseasonal mode supported by our model is a westward traveling dominated by wavenumbers four and five. The oscillation seems to have its highs and lows situated at latitudes about 25 or 30 degrees south, and its features from Australia to South America are much more

stronger than in the rest of the globe. This last characteristic, together with the fact that it has a period of nearly 36 days for $\rho^*=1$, strongly coincide with the 36-40 day mode found in GM.

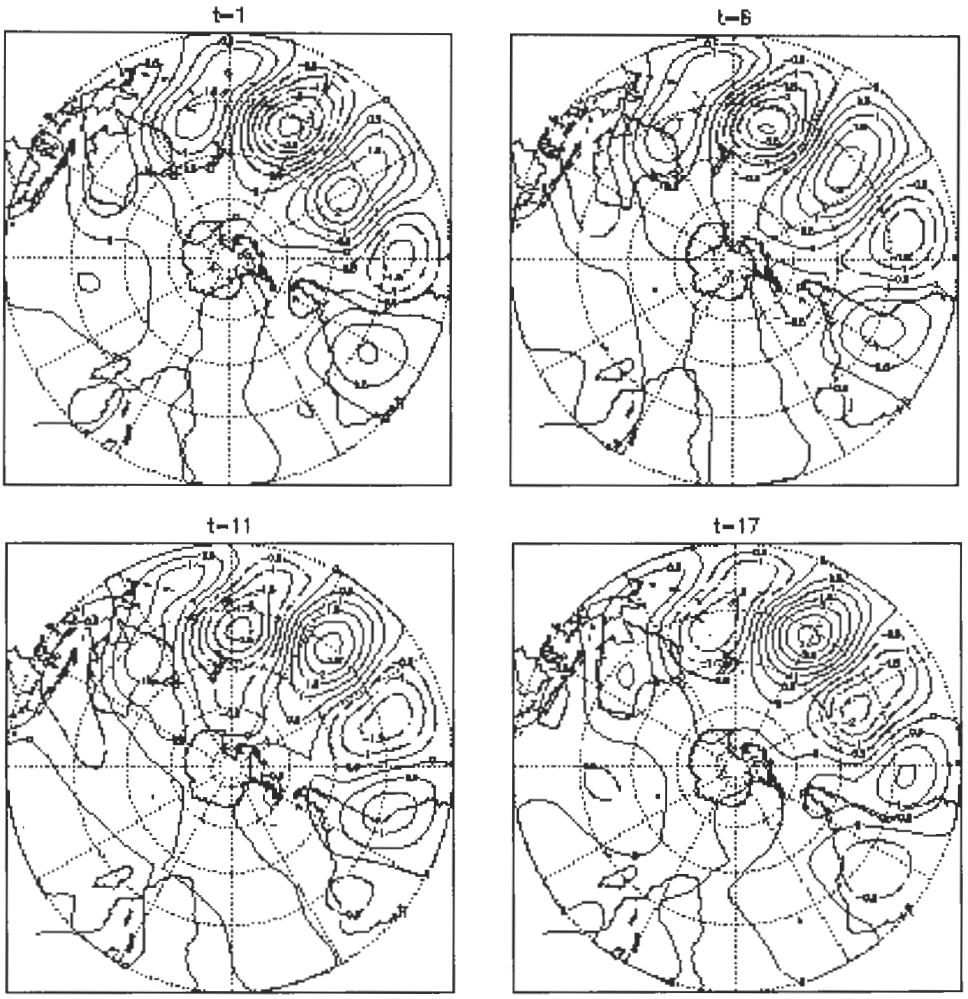

Figure 5- Spatial structure and temporal evolution of half cycle of the intraseasonal unstable mode for $\rho^* = 1.0$. Arbitrary contour values.

However, the intraseasonal mode found in that work, though it has some component of zonal wave number five, is clearly dominated by zonal wave numbers three and four. This difference in wavenumber may be understood following a result of Borges and Sardesmukh (1995). In the model there are two possible instability mechanisms: the topographic instability and the barotropic instability of the non-zonal flow. Since the unstable mode exists even in the absence of topography we associate its appearance as consequence of the barotropic instability. According to the theory of Borgues and Sardesmukh (1995) a perturbation consisting in meridionally elongated eddies (as the unstable mode here) can extract energy only from confluence regions of the basic flow. Looking at Fig. (2) the region of flow convergence off Australia seems to be the regions where the perturbation can get its energy from. Also Borgues and Sardesmukh (1995) pointed out that the spatial scale of the most unstable modes will depend on that of the jet exit, the latter being very sensitive to the choice of the basic state. Thus, although no sensitivity tests were done, we suggest that the difference in wave number between the observational work of GM and ours could be attributed mainly to the sensitivity of the spatial pattern to the chosen basic state.

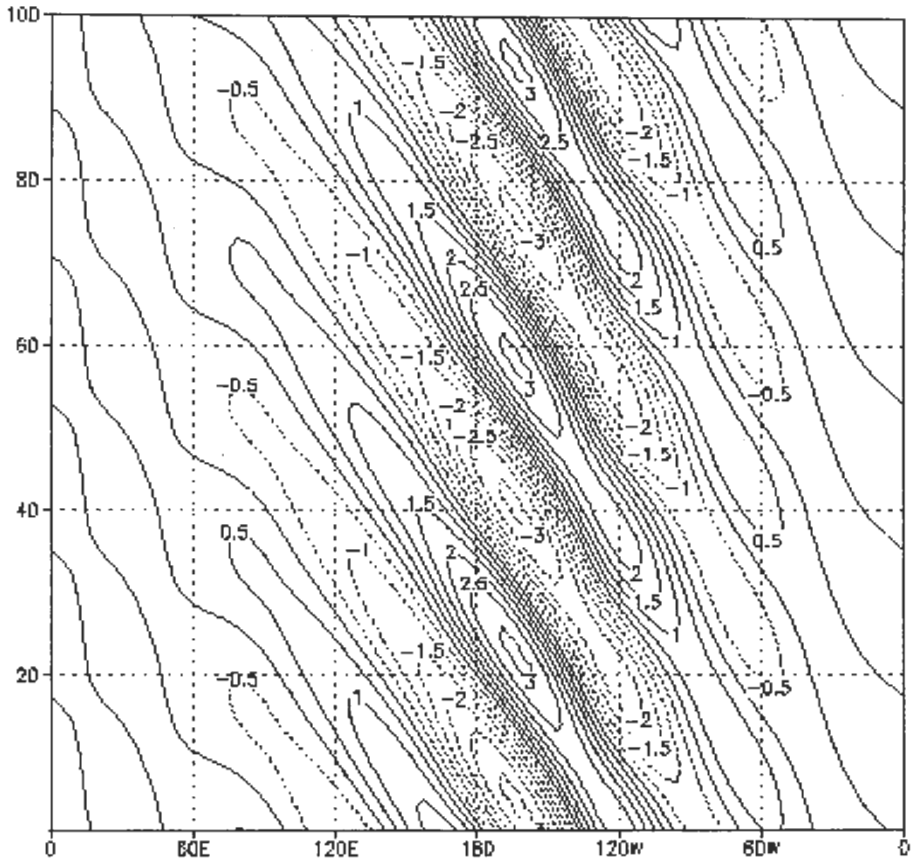

Figure 6- Hovmoller diagram of the unstable mode at 28.5° S for ρ^*=1.0. Ordinate axis is in days.

5. TIME-DEPENDENT SOLUTIONS AND TROPICAL HEATING INFLUENCE

a. Asymptotic behavior

We now consider the time dependent solutions of the model. We focus on the asymptotic behavior integrating the model until it reaches this state. Fig. (7a) shows the total energy of the model as a function of time for a parameter forcing value $\rho^* = 1$. It is clear the existence of a oscillation with small amplitude and with a frequency of 33-34 days as can be seen from the corresponding power spectrum (Fig. (7b)). Thus, the system shows an asymptotic behavior of the same type and characteristics as was found for the unstable intraseasonal mode in the linear stability analysis, with a small shift of the frequency due to nonlinear interactions.

The long term behavior of the model for different values of ρ^* was also performed, being the window of intraseasonal mode instability the same as found by the linear stability analysis. Thus, it can be deduced that the wave created by the Hopf bifurcation at $\rho^* \cong 0.92$ is asymptotically stable in the allowable range. The spatial pattern of oscillatory behavior encountered in this section again resembles the pattern of the 36-40 days intraseasonal mode found in the work of GM.

If we perform the same experiment for January, for the same values of the control parameter, the system goes directly to a steady-state, without any kind of oscillation at all (not shown). This result contradicts the observational fact of the existence of a weak (compared with the wintertime case) intraseasonal oscillation in SH summer. A look at the January forcing streamfunction (not shown) suggests that this may result of its almost zonal structure: in summertime the upper level flow seems to be too zonal for the barotropic instability to generate unstable modes at realistic forcing values. The divergent barotropic model used is not able to detect the energy source for summer modes which would appear as a nonzonal feature in the summer forcing.

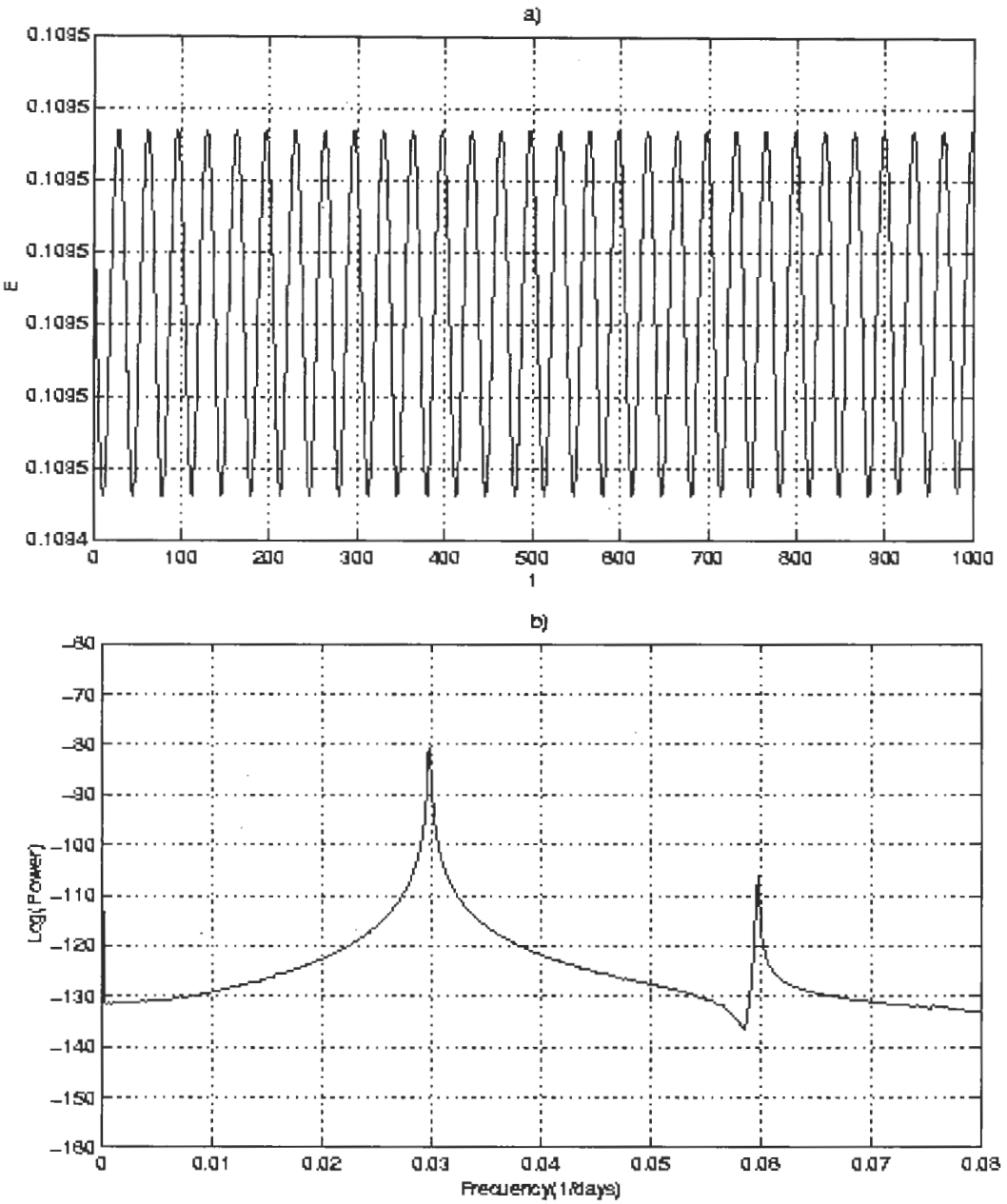

Figure 7- Asymptotic evolution for the model with topography and $\rho^*=\tau=1.0$: a) time series of total energy, and b) corresponding power spectrum.

b. Tropical forcing

In this section a vorticity source is introduced in Eq. (1) to mimic the effects of a tropical oscillatory heating. Following the work of SJG we will now study the possible interactions between this wave (with frequency f^2) and the intraseasonal oscillation (with frequency f^1) induced by the barotropic instability of the non-zonal flow. The control parameter δ, which takes into account the intensity of the heating, is varied to investigate the sensitivity of the system, while ρ * is kept fixed at 1.0. The time evolution of the total energy and its power spectrum are computed as indicators of the system's response when the tropical forcing is allowed to oscillate with periods of 30, 40 or 50 days.

Results show that in all cases both peaks coexists independently on the frequency of the heating source; Figs. (8a) and (8b) show the case for T=30 days. This is

in sharp contrast with the work of SJG where the model did not sustain the two separate oscillations of the tropical and extratropical signals, the latter due to topographic instability, and which was attributed to a type of nonlinear response of the model to the tropical forcing. On the other hand our result agrees with the work of Dickey et al. (1991) where it was found that in the real atmosphere the frequency locking between the tropics and extratropics occurs only seldom.

On the other hand, the coexistence of both frequencies, i.e. f^1 and f^2, in the power spectrum induces a new frequency, $f = |f^1 - f^2|$ by means of nonlinear interaction between the two waves with associated period T =300, 200 and 100 days for $f^2 = 30$, 40 and 50 days^{-1} correspondingly. This new interannual frequency modulates the behavior of the energy, as can be seen from Fig.(8a), as well as the other variables of the system. Thus, in the context of this simple model, the non matching of the intraseasonal tropical and extratropical signals act as a mechanism of creating interannual variability in the SH winter.

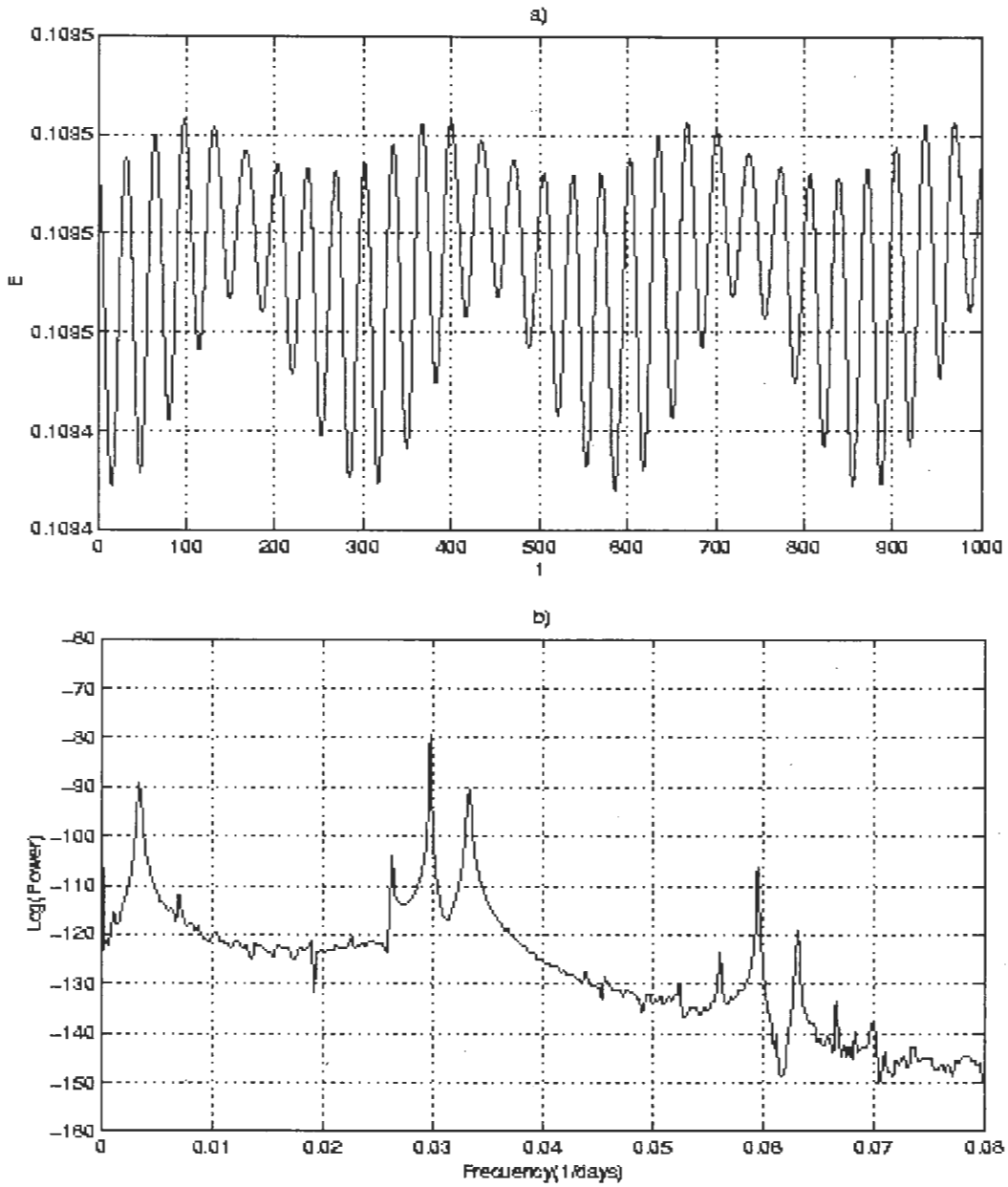

Figure 8- Asymptotic evolution of the model with topography and vorticity source of period T=30 days and $\rho^*=\tau=1.0$: a) time series of total energy, and b) corresponding power spectrum.

6. SUMMARY AND CONCLUSIONS

A nonlinear barotropic quasigeostrophic model was used to study the dynamics of the SH intraseasonal variability. Realistic topography and tropical heating were included as probable sources of intraseasonal variability in the behavior of the model. In the context of this simple model the main results are:

- The presence of topography induces multiple equilibria in the model. On the other hand, and in contrast with the NH case, topography does not have an important role in inducing oscillatory instabilities in the SH winter, which agrees with the suggestion of Kalnay Rivas et al. (1986) in attributing a less important role to topography in the SH low frequency atmospheric dynamics than in the NH case. Moreover if the forcing function is calculated using the summer ECMWF climatology, the model shows a total absence of multiple equilibria even when topography is present, and solutions are all linearly stable.

- The linear unstable intraseasonal mode found has a period of nearly 36 days and an e-folding time of about 125 days for realistic forcing parameter values. It is caused by the barotropic instability of the non-zonal climatological flow and presents common features to observational intraseasonal modes. Although it seems to be a weakly unstable one, it fulfills the same characteristics as the 36-40 days mode found in the observational work of GM for the SH, in terms of the period as well as the spatial structure. It has some similarities in wave number, period and spatial structure to the Pacific South American pattern (PSA), but the PSA shows an eastward propagation and extends further south (Mo and Higgins, 1998). Morevoer, the PSA is associated to enhanced convection in the Pacific ocean (Mo and Higgins, 1998), while the intraseasonal mode found here is the result of the internal dynamics of the extratropical atmosphere.

- To study tropical-extratropical interactions, a vorticity source term was added to the dynamical equation of our model. The results show that, independently of the period considered, the intraseasonal extratropical mode and the tropical one coexist for realistic forcing parameter values. This result coincides with GM in that they did not find any significant relationship between the tropics and the SH intraseasonal variability. Moreover, due to non-linear interactions between the two waves a new signal appears in the range of 100 to 300 days depending on the tropical heating period. Thus, the tropical-extratropical interaction appear in the context of this simple model as essentially two independent events, but at the same time they act as a mechanism of producing interannual variability. This result suggest an interrelation between the intraseasonal and interannual variability scales and stress the independence of extratropical low frequency variability on the intraseasonal scale of the SH winter from the tropical one.

Acknowledgments. The author would like to thank Dr. Fei-Fei Jin for suggesting the topic of the work, useful comments and giving the primary version of the computer code used. This work was partially supported through Proyecto CIC-FI, Universidad de la Republica: "Dinamics of low frequency phenomena in the atmosphere" /95-96.

7-REFERENCES

ANDREWS, D. G. On the stability of forced zonal flows. **Q. J. R. Meteorol. Soc.,** v. 110, p. 657-62, 1984.

BLADE, I., HARTMANN, L. The linear and nonlinear extratropical response of the atmosphere to tropical intraseasonal heating. **J. Atmos. Sci.** v. 52, p. 4448-71, 1995.

BORGES, M. D., SARDESMUKH, P. Barotropic Rossby wave dynamics of zonally varying upper-level flows during northern winter. **J. Atmos. Sci.,** v. 52, p. 3779-96, 1995.

DICKEY, J. O., GHIL, M., MARCUS. S. L. Extratropical aspects of the 40-50 days oscillation in length-of-day and atmospheric angular momentum. **J. Geophys. Res.,** v. 96, n. D12, p. 22643-58, 1991.

GHIL M., MO, K. Intraseasonal oscillation in the global atmosphere. Part I: Northern Hemisphere and Tropics. **J. Atmos. Sci.,** v. 48, p.750-80, 1991a.

GHIL M., MO. K. Intraseasonal oscillation in the global atmosphere. Part II: Southern Hemisphere. **J. Atmos. Sci.**, v. 48, p.780-90, 1991b.

GRIMM, A. M., SILVA DIAS, P. L. Analysis of tropical-extratropical interactions with influence functions of a barotropic model. **J. Atmos. Sci.,** v. 52, p. 3538-55.

GUCKENHEIMER, J., HOLMES, P. **Nonlinear**

oscillations, dynamical systems, and bifurcations of vector fields. Springer-Verlag, 1983. 453p.

JIN, F-F., GHIL, M. Intraseasonal oscillations in the extratropics: Hopf bifurcations and topographic instabilities. **J. Atmos. Sci.** v. 47, p. 3007-22, 1990.

KALNAY, E., MO, K. C., PAEGLE. Inicial Large amplitude, short-scale stationary rossby waves in the Southern Hemisphere: observations and mechanistics experiments to determine their origin. **J. Atmos. Sci.** v. 43, p. 252-75, 1986.

KUBICEK, M., MAREK, M. **Computational methods in bifurcation theory and dissipative structures.** Springer-Verlag, 1983. 243 p.

LAU, K.-M., PHILLIPS, T. J. Coherent fluctuations of extratropical geopotential height and tropical convection in intraseasonal time scales. **J. Atmos. Sci.,** v. 43, p. 1164-81, 1986.

LEGRAS, B., GHIL, M. Persistent anomalies, blocking and variations in atmospheric predictability. **J. Atmos. Sci.,** v. 42, p. 433-71, 1985.

LI, L., NATHAN, T. R. Effects of low-frequency tropical forcing on intraseasonal tropical-extratropical interactions. **J. Atmos. Sci.,** v. 54, p. 332-46, 1997.

MADDEN, R. A., JULIAN, P. R. Detection of a 40-50 day oscillation in the zonal wind of the tropical Pacific. **J. Atm. Sci.,** v. 28, p. 702-8, 1971.

MECHOSO, C. R., FARRARA, J. D., GHIL, M. Intraseasonal variability of the winter circulation in the southern hemisphere atmosphere. **J. Atmos. Sci.** v. 48, p.1387-404, 1991.

MO, K., HIGGINS, R. W. The Pacific-South American modes and tropical convection during the southern hemisphere winter. **Mon. Wea. Rev.** v.126, p.1581-96, 1998.

ROSEN R., SALSTEIN, D. A. Variations in atmospheric angular momentum on global and regional scales and length of day. **J. Geophys. Res.,** v. 96, p. 5145-51, 1983.

SIMMONS, A. J., WALLACE, J. M., BRANSTATOR, G. W. Barotropic wave propagation and instability, and atmospheric teleconnection patterns. **J. Atmos. Sci.,** v. 40, p. 1363-92, 1983.

STRONG, C. M., JIN, F-F., GHIL, M. Intraseasonal variability in a barotropic model with seasonal forcing. **J. Atmos. Sci.,** v. 50, p. 2965-86, 1993.